Neurochem Res (2017) 42:1288–1298
DOI 10.1007/s11064-016-2170-z

ORIGINAL PAPER

Reversal of TRESK Downregulation Alleviates Neuropathic Pain by Inhibiting Activation of Gliocytes in the Spinal Cord

Jun Zhou[1] · Hongtao Chen[2] · Chengxiang Yang[1] · Jiying Zhong[1] · Wanyou He[1] · Qingming Xiong[1]

Received: 20 August 2016 / Revised: 3 November 2016 / Accepted: 28 December 2016 / Published online: 3 February 2017

Abstract Despite the consensus that activation of TWIK-related spinal cord K^+ (TRESK) might contribute to the pathogenesis of chronic pain, the specific mechanisms underlying the transfer and development of pain signals still remain obscure. In the present study, we validated that TRESK was expressed in neurons instead of glial cells. Furthermore, in the SNI model of neuropathic pain (NP), downregulation of TRESK in spinal cord neurons resulted in upregulation of connexin 36 (Cx36) and connexin 43 (Cx43), both being subtypes of gap junctions in the spinal cord, with gliocytes in the spinal cord activated ultimately. Compared with SNI rats, intrathecal injection of TRESK gene recombinant adenovirus significantly downregulated the expression levels of Cx36 and Cx43 and suppressed the activation of gliocytes in the spinal cord, with hyperalgesia significantly reduced. In conclusion, TRESK contributes to the pathogenesis of NP by upregulation of synaptic transmission and activation of gliocytes.

Keywords TRESK · Gap junction · Spinal cord · Gliocyte · Neuropathic pain

✉ Hongtao Chen
gz8hcht@126.com

[1] Department of Anesthesiology, First People's Hospital of Foshan, Foshan, Guangdong Province 528000, China

[2] Department of Anesthesiology, Eighth People's Hospital of Guangzhou, Guangzhou, Guangdong Province 510060, China

Introduction

Neuropathic pain (NP) is a public health problem worldwide [1]. Potassium channel changes that cause abnormal discharges are important physiological factors that lead to NP [2, 3]. The TWIK-related spinal cord K^+ (TRESK) channel, a two-pore domain potassium channel, produces a cell background potassium current that is closely related to the onset and development of various chronic pain conditions [4–6]. Due to its unique attributes, an increasing number of studies have regarded TRESK as an important factor in the pathogenesis of NP [4, 7]. However, the specific mechanisms underlying TRESK-mediated NP are incompletely understood.

Gliocytes account for over 70% of the cell population in the central nervous system (CNS) and are classified into astrocytes, oligodendrocytes and microglia. Activation of microglia and astrocytes contributes to dramatic changes in various genes, including cell-surface receptors that participate in neurotransmission, intracellular signaling molecules and bioactive diffusible factors, thus playing important roles in NP pathogenesis [8–11]. Moreover, synaptic transmission plays an important role in pain signaling [12]. TRESK is mainly expressed in the dorsal root ganglia (DRG) and spinal cord [13]. In the current study, we validated the TRESK-specific distribution and demonstrated that TRESK-mediated synaptic transmission might play a bridge role in pain signal transmission from spinal cord neurons to gliocytes in NP rats.

Electrical signaling and intercellular exchange of small molecules including ions and second messengers are transmitted by gap junctions which connect opposing cells, either neurons or glia, through connexin (Cx) protein subunits [14]. Over 20 Cx genes are identified and characterized in the immature and adult central nervous

systems (CNS). Increasing evidence indicates that alterations in the expression and activity of gap junction channels in the spinal cord are involved in the development of neuropathic pain [12]. In the spinal cord, expression of neuronal Cx proteins such as Cx36 and of glial subtypes including Cx43 is established [15, 16].

On the grounds of our recent findings that upregulated TRESK expression in SNI rats significantly decreased hyperalgesia [17, 18], we investigated the role of TRESK in synaptic transmission and gliocytes-mediated NP using gene recombinant adenovirus.

Materials and Methods

Animals

Adult male Sprague–Dawley rats (weighing 250–280 g, the Laboratory Animal Center of the First People's Hospital of Foshan, Foshan, China) were randomly allocated to standard cages with 4 or 5 animals per cage. The environment was maintained at a constant temperature (22 ± 0.581 °C) and relative humidity (60 ± 70 %) with a 12-hour light/dark cycle (lights on at 7 a.m.). All animals were fed on a standard laboratory diet with *ad libitum* access to tap water. The animals were housed in the experimental room for 24-hour acclimation prior to behavioral testing.

Implantation of the Intrathecal Catheter

The animals underwent a chronical intrathecal cannulation [19] 1 week prior to SNI surgery or intrathecal injections of the virus and inhibitor. With the skin incised from the posterior nuchal area at the scalp, and the occipital muscle was separated from the attached portion on the back of the base of the skull under sodium pentobarbital anesthesia (45 mg/kg, intraperitoneally). A polyethylene catheter (PE-10, 8.0 cm) was advanced from the cisternal membrane to the region of lumbar enlargement and was externalized at the back of the head. Recovery from anesthesia after intrathecal catheter implantation, upper segments of the spinal cord were checked to resulting healthy. Lidocaine (2%, 20 μl) was intrathecally administered via the catheter on the second day, and rats which exhibited double lower limb paralysis within 30 s and recovered within 30 min were considered to have undergone successful intrathecal cannulation, and thereafter were randomized for the subsequent experiment, which involved intrathecal injection of the adenovirus.

SNI

Rats with successful intrathecal cannulation underwent SNI surgery [20] under anesthesia. The rats were fixed to an operating table, with the femur at the right mid-thigh level as the incision landmark. The 3 peripheral branches (the sural, common peroneal, and tibial nerves) of the sciatic nerve were exposed at mid-thigh level distal to the trifurcation without stretching of the nerve structures and were freed of connective tissue. The tibial and common peroneal nerves were tightly ligated by two knots, 4 mm apart, using 6–0 silk sutures (Ethicon, Johnson & Johnson Inc., Brussels, Belgium) and were then completely severed between the knots. The sural nerve was left intact by meticulous avoidance of any nerve stretching or contact with surgical instruments. The muscle and skin were closed in 2 distinct layers using 5–0 silk sutures [21]. The sham group underwent the identical procedures except nerve ligation and transection.

Nociceptive Behavior

All behavioral tests were conducted in a blinded manner. Nociceptive responses to mechanical and thermal stimuli were measured 3 h prior and 1, 3, 5 and 7 days subsequent to surgery.

Mechanical Allodynia

Mechanical withdrawal thresholds (MWTs) were measured with von Frey filaments (Stoelting, Wood Dale, Illinois, USA) applied to the right hind paw until a positive sign of pain behavior was elicited [22]. The test area included the mid-plantar paw in the distribution area of the sciatic nerve. Von Frey filaments with logarithmically incremental stiffness (0.4–15.1 g) were serially applied to the paw using the up-down method. The filaments were presented in ascending order of strength, perpendicular to the plantar surface, with sufficient force to cause slight bending against the paw, and they were held for 6–8 s. A positive response was noted if the paw was sharply withdrawn. Flinching immediately upon removal of the hair was also considered a positive response. The 15.1 g filament was selected as the upper cutoff for testing, and in the absence of response, the 15.1 g filament was assigned as cutoff value. The bending force that evoked 50% of paw withdrawal occurrence was set as the MWT.

Hargreaves Plantar Test

The Hargreaves test was used to measure paw thermal withdrawal latency (TWL) to heat stimuli and to determine the presence of thermal hyperalgesia [23]. The rat was placed

on the surface of a 2-mm-thick glass plate covered with a plastic chamber (20×20×25 cm). TWL was measured using a radiant thermal stimulator (BME410A, Institute of Biological Medicine, Academy of Medical Science, Tianjin, China). Heat was concentrated on the hind paw, flush against the glass, and radiant heat stimulation was delivered to the site. The stimulus terminated with hind paw movement, and a 25 s cutoff was used for the stimulus duration to obviate tissue damage. The intensity of thermal stimulation remained constant throughout the experiment. Five stimuli were applied to the same site, and the mean TWL was obtained from three thermal stimulations and used as the TWL value of the steady state.

Drug Administration

TRESK gene recombinant adenovirus (pAd/CMV/V5-DEST-TRESK, 1×10^9 IFU/ml) (Ruisai Co., Ltd., Shanghai, China) was dissolved in normal saline prior to experiment. The adenovirus or the corresponding negative adenovirus was intrathecally injected (10 µl) once daily for 7 consecutive days.

Western Blot Analysis

Protein was extracted from spinal cord tissue using a radioimmunoprecipitation assay buffer containing cocktail proteinase inhibitors (Sigma) and was quantified with a Bio-Rad protein assay. An equal amount of protein was separated on SDS–polyacrylamide gels in a Tris/HCl buffer system, transferred onto nitrocellulose membranes, and blotted according to standard procedures with primary antibodies (TRESK, Iba I, and GFAP) (Cell Signaling Technology, Danvers, MA, USA). Membranes were then stripped and reblotted with anti-GAPDH (Santa Cruz Biotechnology, Santa Cruz, CA, USA). The specific bands of target proteins were visualized by chemiluminescence, and the band intensities were quantified using NIH ImageJ software.

Quantitative Real-time RT-PCR

Quantitative analysis of the target mRNA expression was performed with real-time RT-PCR by the relative standard curve method. Total RNA was extracted from snap-frozen spinal cord tissues with TRIzol Reagent (Invitrogen), followed by treatment with RNase-free DNase I (Roche). Aliquots (1 µg) of total RNA were reverse transcribed and amplified in triplicate using IQ SYBR Green Supermix reagent (Bio-Rad, Hercules, CA, USA) with an Opticon real-time PCR machine (MJ Research, Waltham, MA, USA), according to the manufacturers' instructions. The specificity of real-time PCR was confirmed via routine agarose gel electrophoresis and melting-curve analysis. The following primer sequences were used: TRESK -forward, 5′-GGT GCCAACGATGATCT-3′, reverse, 5′-CTGCTGGGCTGT GGGTCTAG-3′; Cx36-forward, 5′-CATAATGGTGTG TACCCCCAGTCT-3′, reverse, 5′-CGGCGTTCTCGC TGCTT-3′; Cx43-forward, 5′-TACCACGCCACCACT GGCCCA, reverse, 5′- CTAAAGGGGCTGCTGTTGGTC TTA-3′ and GAPDH-forward, 5′-TGCTGAGTATGTCGT GGAGTCTA-3′, reverse, 5′-AGTGGGAGTTGCTGTTGA AATC-3′. The expression level of TRESK mRNA and CX43 mRNA was normalized to the GAPDH level in each sample.

Immunofluorescence

$L_{4–5}$ DRG and spinal cord paraffin-embedded sections were dewaxed and quenched with 3% H_2O_2. Nonspecific binding was blocked with serum-free protein block (DAKO). The slides were then incubated with anti- connexin 36 (Cx36), connexin 43 (Cx43), Iba I, GFAP, Neu N and TRESK antibodies (Rockland), followed by incubation with Alexa-594 antibodies (Invitrogen). Cx36 and Cx43 were individually stained in the spinal cord for immunofluorescence. Neu N, Iba and GFAP were restained with TRESK. The slides were mounted with VECTASHIELD Hard Set mounting medium with DAPI. Fluorescence intensity was visualized using a confocal or deconvolution microscope equipped with a digital camera (Nikon, Melville, NY, USA). Quantitative evaluation of the sections stained with antibodies was performed using NIS-Elements Br software, version 3.0. The fluorescence-positive area was calculated as a percentage of the total area.

Statistical Analysis

The data are presented as the means ± SEM. The results from the behavioral study, real-time PCR, western blot and immunohistochemistry evaluations were statistically analyzed using one-way or two-way analysis of variance (ANOVA). Pair-wise comparisons between the means were analyzed using the Newman-Keuls comparison test. Significance was set at $p<0.05$.

Results

Nociceptive Behavior Developed in SNI Model Rats

The nociceptive behavior was determined in SNI model. The ipsilateral hind paws of SNI rats showed a decrease in the MWT at 1, 3, 5 and 7 days (Fig. 1a). SNI modeling did not modify the thermal allodynia in the rats at any of the time points (Fig. 1b).

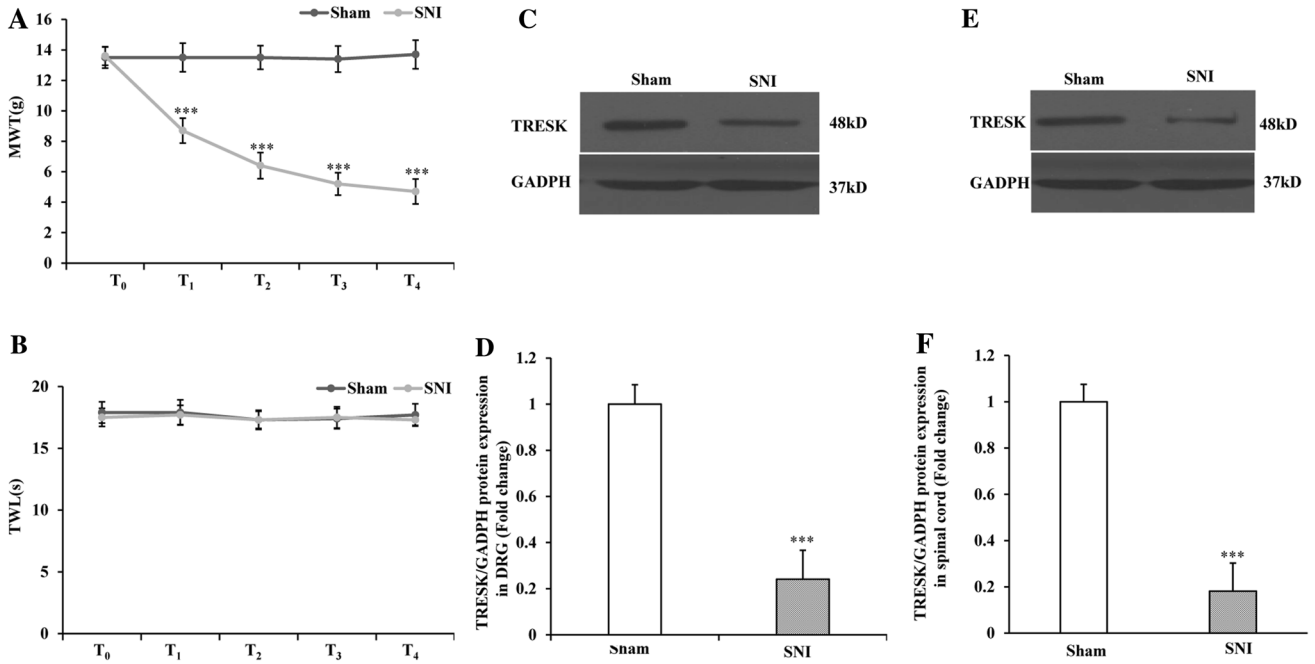

Fig. 1 Nociceptive behavior developed and TRESK expression in SNI model rats. **a** MWT (mechanical withdrawal threshold) at each time point. **b** TWL (thermal withdrawal latency) at each time point. ***p < 0.001 compared to the Sham group. **c** Representative western blots showing TRESK protein expressions in DRG of Sham and SNI rats. **d** Quantitative analysis of TRESK protein expressions in DRG of Sham and SNI rats. **e** Representative western blots showing TRESK protein expression in spinal cord of Sham and SNI rats. **f** Quantitative analysis of TRESK protein expressions in spinal cord of Sham and SNI rats. ***$p < 0.001$ versus the Sham group ($n = 6$ each)

Changes in TRESK Expression and Distribution in the DRGs and Spinal Cords of SNI Rats

Western blot analysis showed that the protein levels of TRESK were downregulated in DRG and spinal cord from SNI rats compared with Sham rats at 7 days (Fig. 1c, d, e, f). Due to a paucity of literature regarding the distribution of TRESK in DRG and the spinal cord in the SNI model, we examined the distribution of TRESK by immunofluorescence. The results of neuron marker (Neu N) and TRESK counterstaining showed that TRESK was abundantly expressed in the neurons in normal rat DRGs and spinal cords (Fig. 2). Astrocyte markers and microglial markers restained with TRESK showed that TRESK was not expressed in gliocytes from normal rats (Fig. 3).

Effect of pAd/CMV/V5-DEST-TRESK on Nociceptive Behavior in SNI Rats

In light of our previous study that TRESK gene recombinant adenovirus (pAd/CMV/V5-DEST-TRESK, 1×10^9 IFU/ml) effectively upregulated TRESK expression [18], to explore the effects of TRESK on NP pathogenesis, normal rats were randomized into four groups ($n = 6$ each), which received sham, SNI model, SNI model and intrathecal injection with TRESK-overexpressing adenovirus and SNI model and intrathecal injection with negative adenovirus treatments, respectively, hence the designation of sham group, SNI group, SNI-TRESK-AdV group and SNI-AdV group. All SNI model rats developed mechanical allodynia ipsilaterally at $T_{1–7}$, which was significantly reduced in rats receiving pAd/CMV/V5-DEST-TRESK (Fig. 3a). SNI modeling did not modify thermal allodynia in the rats at any of the time points (Fig. 3b).

Effect of pAd/CMV/V5-DEST-TRESK on TRESK Expression in the DRG and the Spinal Cords of SNI Rats

Based on our previous study that intrathecal pAd/CMV/V5-DEST-TRESK upregulated TRESK expression in SNI rats, the expressions of TRESK in the DRG and the spinal cord were determined by real-time PCR for further authentication. As shown in Fig. 4c, d TRESK expressions in the DRG and spinal cord were significantly downregulated in the SNI group and SNI- Adv group verse the sham group ($p < 0.05$, $n = 6$). Intrathecal injection of pAd/CMV/V5-DEST-TRESK significantly upregulated TRESK expressions in the DRG and the spinal cord vs. the SNI group.

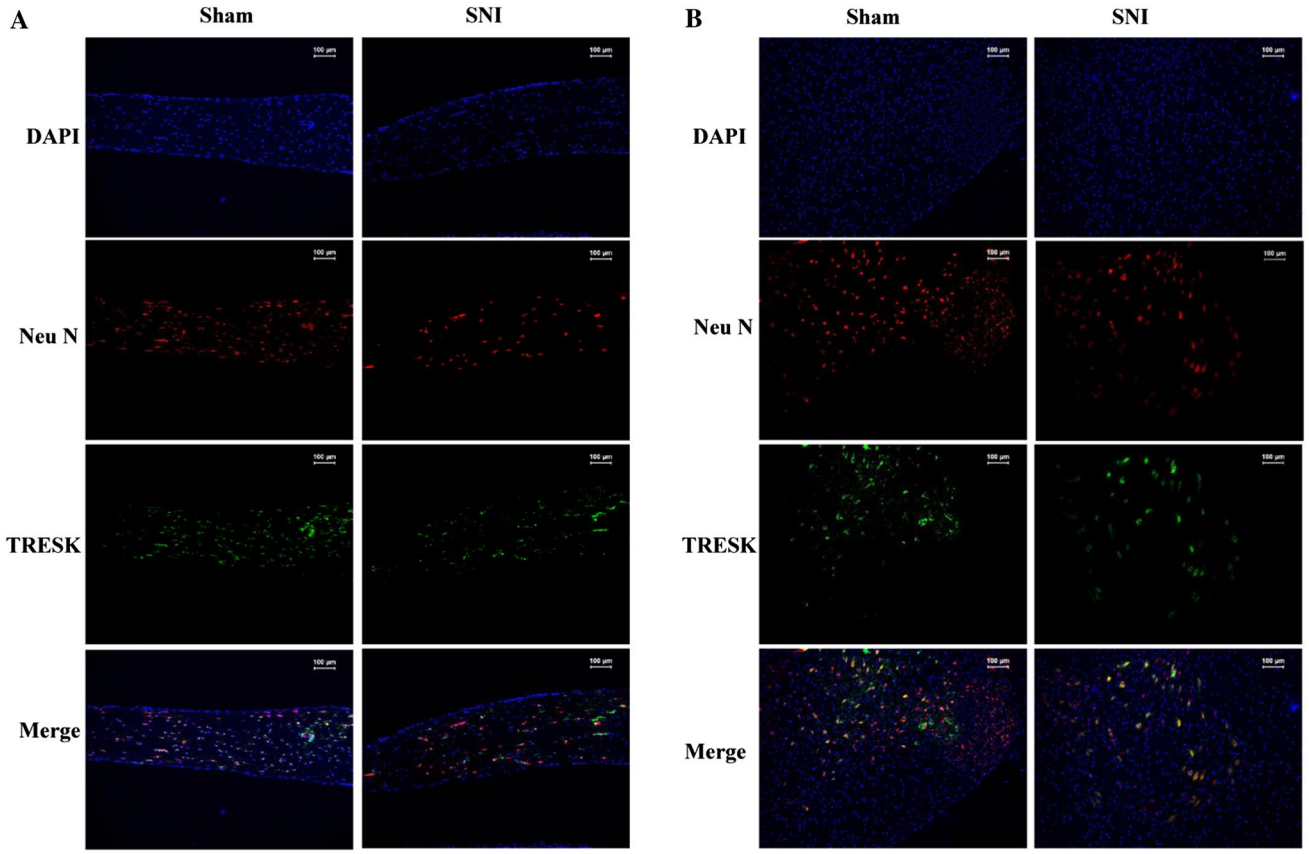

Fig. 2 TRESK expression in neurons in the DRG and spinal cord in SNI rats. Results of neurons markers (Neu N) and TRESK counterstaining showed that TRESK were abundantly expressed in neurons in DRG (**a**) and spinal cord (**b**) in normal rats

Effect of pAd/CMV/V5-DEST-TRESK on Activated Gliocytes in SNI Rats

Our previous studies prompted that pAd/CMV/V5-DEST-TRESK could inhibit astrocyte activation in the spinal cords of SNI rats [18]. Astrocytic and microglial activation in the spinal cord were further verified by western blot and immunofluorescence in our present study, which validated the effects of the downregulation of TRESK overexpression on activated astrocytes in the spinal cords of SNI rats. Compared with the sham group, the population of activated astrocytes in the spinal cord was significantly increased in the other groups of rats undergoing SNI surgery, and intrathecal injection of pAd/CMV/V5-DEST-TRESK significantly depopulated the activated astrocytes in the spinal cord vs. the SNI group (Fig. 5a, b). To explore the effects of TRESK on the microglia and its origin in the spinal cord in SNI rats, activated microglia in the spinal cords from SNI rats were observed. As compared to the sham group, activated microglia in the spinal cord were significantly multiplied in the other groups of rats subjected to SNI surgery. Intrathecally injected pAd/CMV/V5-DEST-TRESK significantly downsized the activated microglia in the spinal cord vs. the SNI group (Fig. 5c, d).

Effect of pAd/CMV/V5-DEST-TRESK on Cx36 and Cx43 Expression in SNI Rats

We observed that the downregulation of TRESK-activated astrocytes in the spinal dorsal horns from SNI rats, despite the abundantly expressed TRESK in the neurons rather than gliocytes. Upregulation of gap junctions has been shown to not only involve in activation of glial cells, but also realize remote connected communication between gliocytes and neurons, and influence excitability and spontaneous discharge of adjacent sensory neurons in NP. Therefore, We detected the influence of TRESK change on gap junctions in SNI rats [24, 25]. Cx36 is principally associated with neuronal gap junctions distributed throughout the adult CNS [15]. Therefore, we examined Cx36 expression in spinal cords harvested 7 days after pain behavior detection. The expression of Cx36 was significantly upregulated in the ipsilateral L_{4-5} spinal cord dorsal horn in SNI rats. Cx36 expression was downregulated in the ipsilateral spinal cord dorsal horn of the SNI-TRESK-AdV rats vs. the

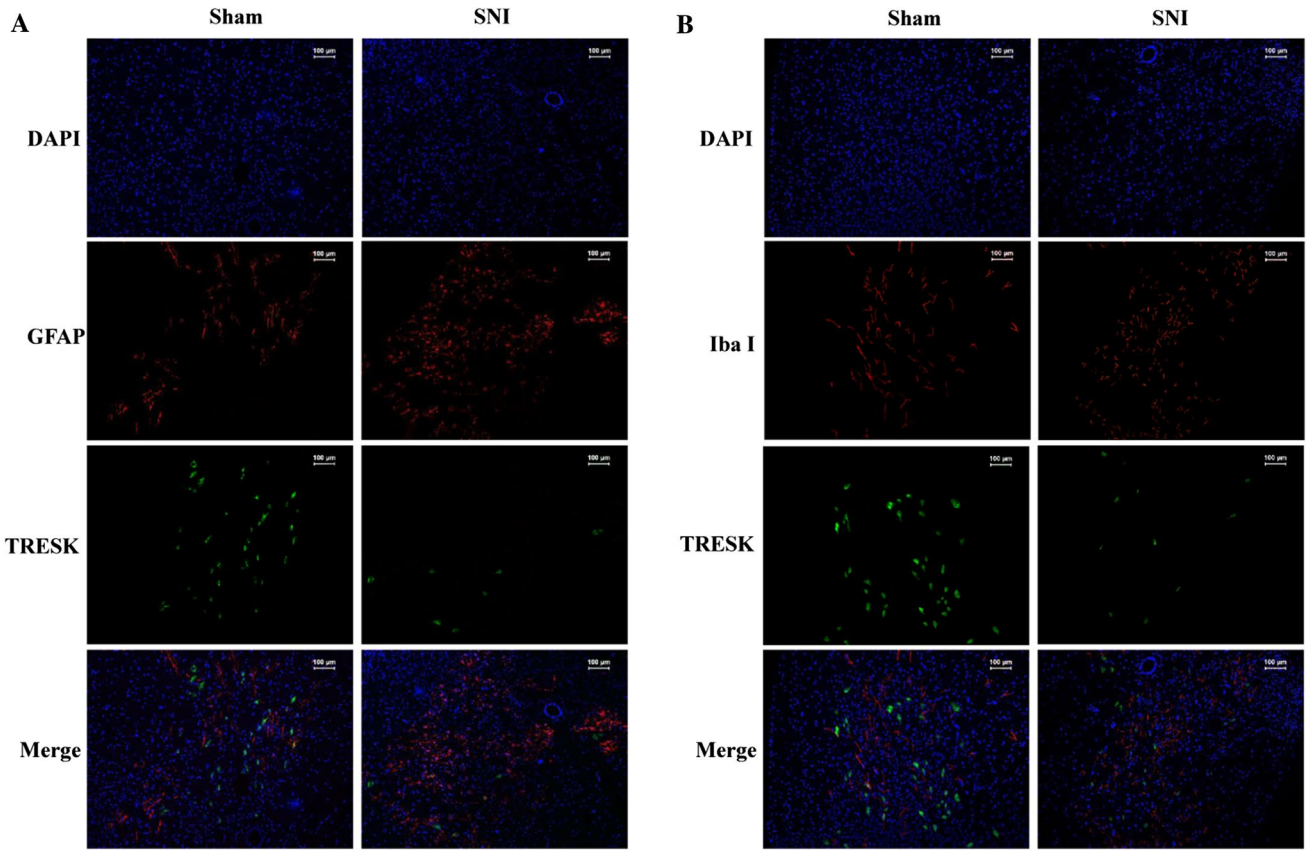

Fig. 3 TRESK expression in gliocytes in the spinal cord in SNI rats. Astrocyte marker and microglial marker were redyed respectively with TRESK in spinal cord. TRESK was not expressed in astrocytes (**a**) and microglia (**b**) in rats

SNI rats. However, no difference was evidenced in Cx36 expression in the ipsilateral lumbar spinal cord between the SNI group and the SNI-AdV group (Fig. 6). Accordingly, we assessed Cx43 expression in spinal cords harvested 7 days after pain behavior detection. The expression of Cx43 was significantly upregulated in the ipsilateral L_{4-5} spinal cord dorsal horn in SNI rats. Cx43 expression was downregulated in the ipsilateral spinal cord dorsal horn in the SNI-TRESK-AdV rats versus the SNI rats. No difference was witnessed in Cx43 expression in the ipsilateral lumbar spinal cord between the SNI group and the SNI-AdV group whatsoever (Fig. 7).

Discussion

Our study has demonstrated that TRESK is mainly expressed by neurons, which contributes to the pathogenesis of NP via the activated gliocytes and upregulation of gap junctions.

The expression and distribution of TRESK in the DRG and spinal cord horn were determined in our study. Upregulation of TRESK expression reportedly reduces the excitability of trigeminal ganglion nociceptors [26], and TRESK in the DRG is significantly downregulated in various pain models [4, 27, 28], whereas the expression and distribution of TRESK in the spinal cord require further clarification. We confirmed that a large amount of TRESK was expressed in neurons rather than gliocytes. Moreover, our data suggested that the variations in TRESK in the spinal cord horn were in line with those in the DRG, and TRESK was remarkably downregulated in the SNI model. Contrary to our study, there is a report that TRESK expression was increased in the rat spinal cord in an NP model [13]. This discrepancy might be attributable to distinctions in pain models or the molecular methods involved. Our study affirmed the involvement of TRESK in NP mechanisms. Our findings are also supported by the reports that TRESK-overexpressing adenovirus (pAd/CMV/V5-DEST-TRESK) could upregulate TRESK expression in the DRG and reverse established tactile allodynia in SNI rats [17, 18]. Our data showed that pAd/CMV/V5-DEST-TRESK also effectively validated SNI-induced downregulation of TRESK.

An increasing number of studies have indicated that spinal gliocytes (astrocytes and microglia) are activated in

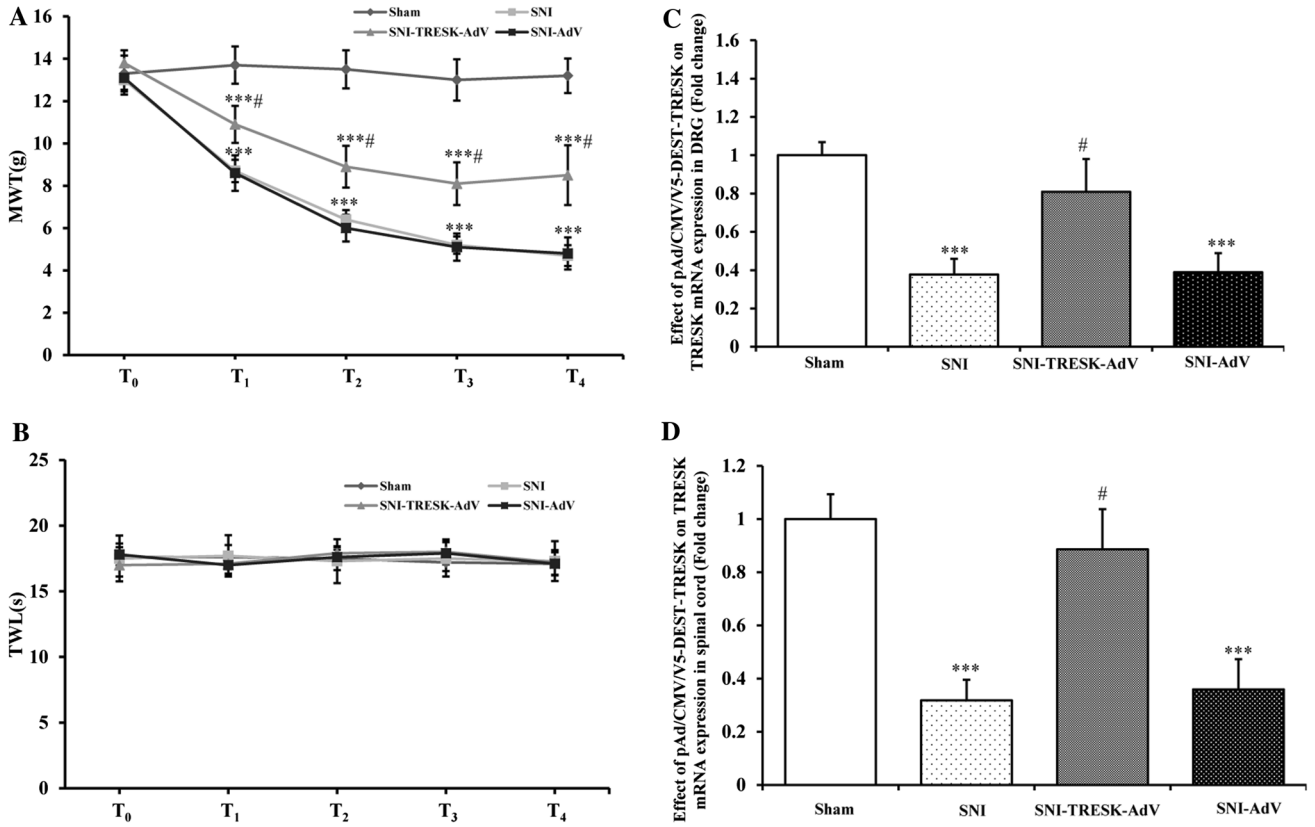

Fig. 4 Effects of pAd/CMV/V5-DEST-TRESK on nociceptive behavior and TRESK expressions in SNI rats. All SNI model rats developed mechanical allodynia ipsilaterally at T_{1-7} versus sham group (***$p<0.001$, $n=6$); PAd/CMV/V5-DEST-TRESK significantly reduced mechanical allodynia ipsilaterally at T_{1-7} in SNI-TRESK-AdV group versus SNI group ($^{\#}p<0.05$, $n=6$) (**a**). Thermal allodynia was not modified in SNI rats at any time point (**b**). TRESK expressions in DRG and spinal cord detected by real-time PCR were significantly downregulated in SNI group and SNI-AdV group versus sham group (***$p<0.001$, $n=6$); Intrathecal injection of pAd/CMV/V5-DEST-TRESK significantly upregulated TRESK expressions in DRG and spinal cord vs. SNI group ($^{\#}p<0.05$, $n=6$) (**a**) and (**b**)

animal models of chronic pain [29–32]. Our previous study also preliminarily showed that TRESK might be associated with astrocyte activation in the spinal cords of SNI rats [18]. Therefore, our study demonstrated the degree of activation of astrocytes and microglia in the spinal cords from SNI rats, confirming that downregulation of TRESK resulted in gliocyte activation in the spinal cord, which is involved in NP pathogenesis. Reversal of SNI-induced downregulation of TRESK via an intrathecal injection of a TRESK-overexpressing adenovirus could mitigate NP conditions by suppressing activation of glial cells in the spinal cord.

Glia-neuron interactions play pivotal roles in the development of NP [33]. Connexin (Cx) proteins and gap junctions support the formation of neuronal and glial syncytia that are linked to different forms of rhythmic firing and oscillatory activity in the central nervous system. We speculated that gap junctions might involve in TRESK downregulation in neurons and activation of gliocytes in the NP pathogenesis [34, 35].

Cx36 is principally associated with neuronal gap junctions and Cx43 is localized to gap junctions between astrocytic processes and oligodendrocytes [36–38]. Kay CW proved that the physiological role for Cx36 and Cx43 in rhythmic firing in the key nociceptive processing area of dorsal horn in the recent study [39]. Cx36 expression was markedly reduced, with the time course of change paralleling the emergence of tactile allodynia after a peripheral nerve injury, and this effect could be mimicked by injection of Cx36 siRNA to knock down Cx36 expression [40]. Cx43 is upregulated and suppression of spinal Cx43 expression inhibited injury-induced mechanical hypersensitivity after L5 spinal nerve ligation [41]. Thus, we evaluated the expressions of Cx36 and Cx43 in the spinal cord, suggesting the expressions of Cx36 and Cx43 were significantly upregulated in SNI rats, which was consistent with our hypothesis.The results demonstrated that astrocytes and gap junctions were activated by TRESK downregulation in the neurons of the spinal cord, which mediates the occurrence and maintenance of NP.

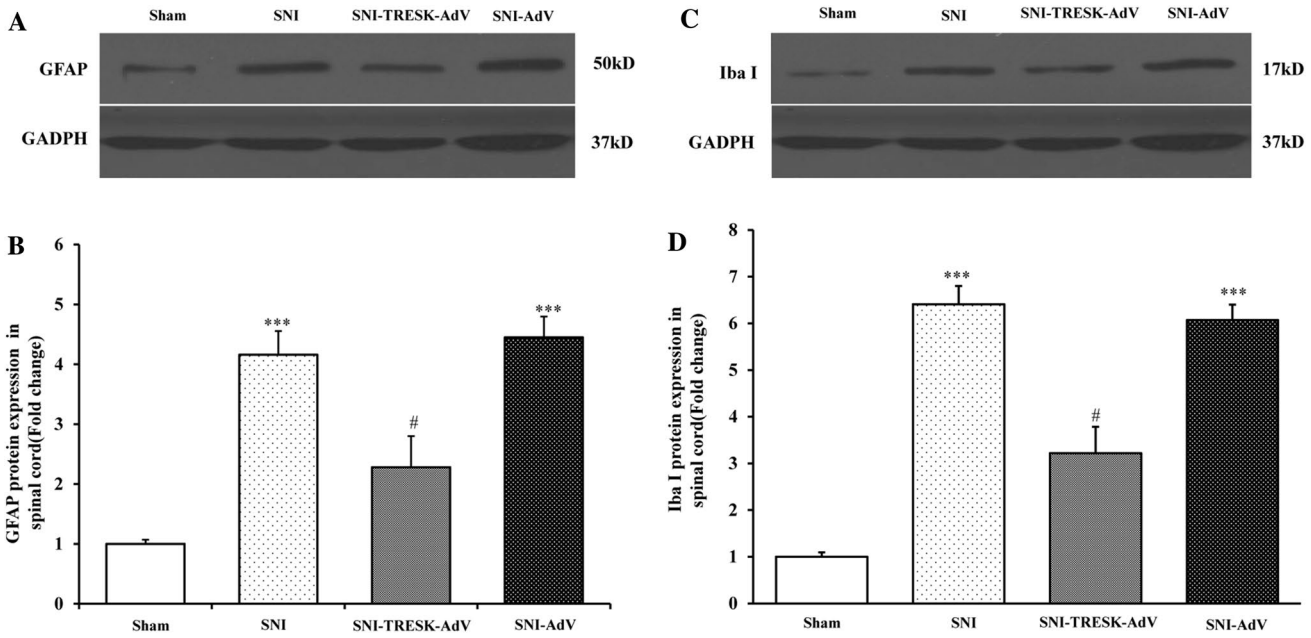

Fig. 5 Effects of pAd/CMV/V5-DEST-TRESK on activated gliocytes in SNI rats. Representative western blot showing GFAP (**a**) and Iba I (**c**) protein levels in SNI rats after pAd/CMV/V5-DEST-TRESK or negative adenovirus treatment. Compared with Sham group, activated astrocytes in spinal cord were increased significantly in other groups undergoing SNI surgery (***$p<0.001$, $n=6$), intrathecal injection of pAd/CMV/V5-DEST-TRESK significantly decreased activated astrocytes in spinal cord versus SNI group ($^{\#}p<0.05$, $n=6$) (**b**). Compared with Sham group, activated microglia in spinal cord were increased significantly in other groups subjected to SNI surgery (***$p<0.001$, $n=6$). Intrathecal injection of pAd/CMV/V5-DEST-TRESK significantly decreased activated microglia in the rat spinal cord vs. SNI group ($^{\#}p<0.05$, $n=6$) (**d**)

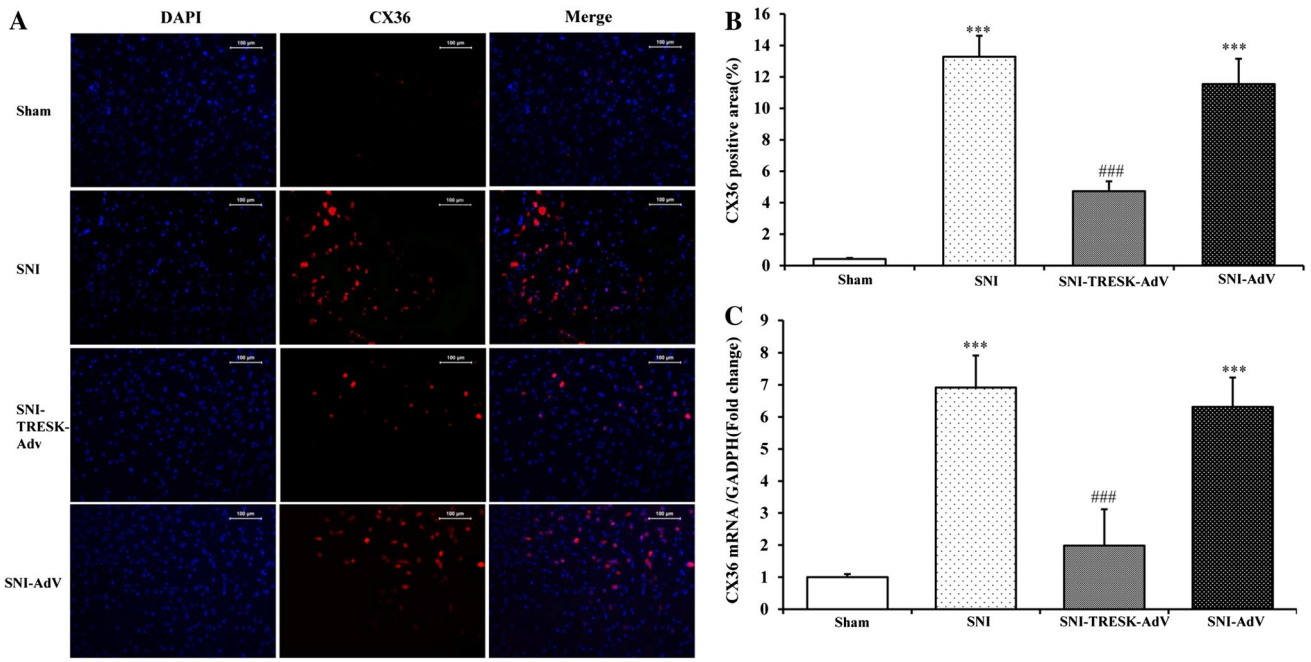

Fig. 6 Effects of pAd/CMV/V5-DEST-TRESK on Cx36 expressions in SNI rats. In the ipsilateral L_{4-5} spinal cord dorsal horn, the Cx36 expression was significantly upregulated in SNI-injured rats (***$p<0.001$, $n=6$). Cx36 expression was downregulated in the ipsilateral spinal cord dorsal horn of SNI-TRESK-AdV group vs. SNI rats ($^{\#\#\#}p<0.001$, $n=6$)

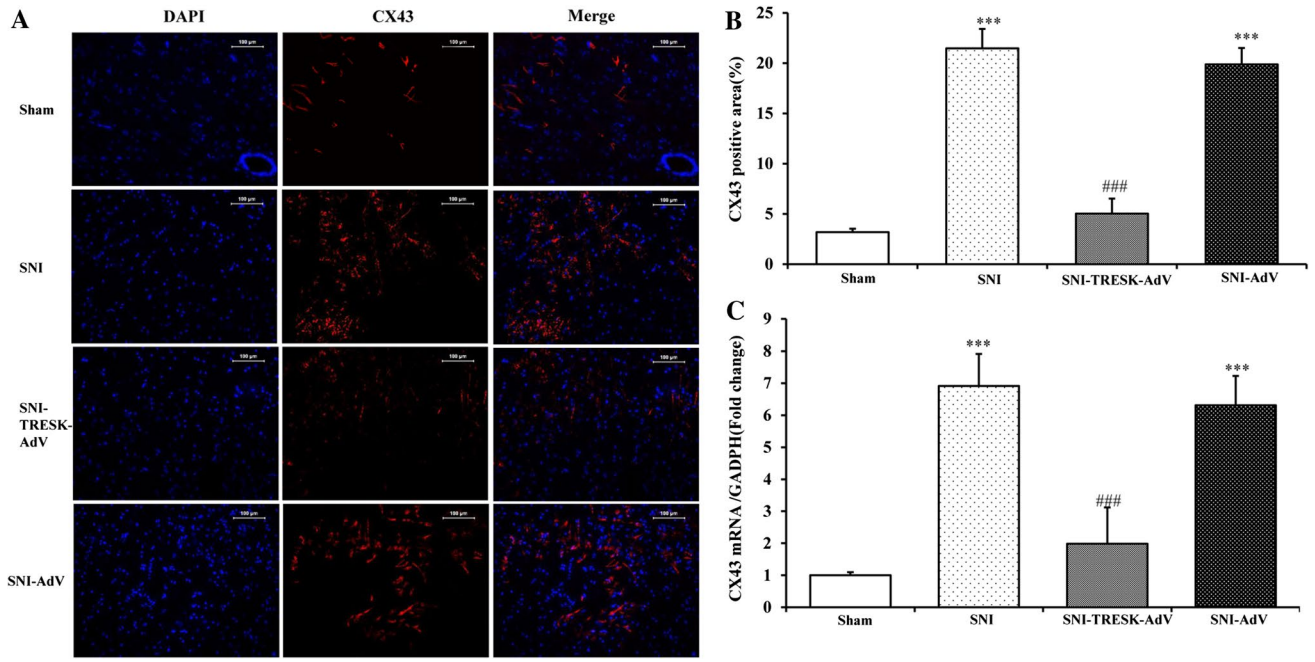

Fig. 7 Effects of pAd/CMV/V5-DEST-TRESK on Cx43 expression in SNI rats. In the ipsilateral L_{4-5} spinal cord dorsal horn, the Cx43 expression was significantly upregulated in SNI-injured rats (***$p<0.001$, $n=6$). Cx43 expression was downregulated in the ipsilateral spinal cord dorsal horn in SNI-TRESK-AdV group vs. SNI rats (###$p<0.001$, $n=6$)

We detected gap junctions expression of spinal cord in rats at 7 days after SNI, it prove that activation of gliocytes and upregulation of gap junctions involved in TRESK mediated mechanism of NP. In fact, gliocytes activation and gap junctions played an important role in the early and the first phase of NP progression, especial for the microglia. In the presence of nerve damage or other incentives, abnormal release of neurotransmitters, cytokines and so on from neurons could affect the expression of connection protein and the permeability of gap junctions [42]. The increase of gap junctions participated in the process of gliocytes activation, and the activation of gliocytes induced to central sensitization and inflammatory factors release, further effect on neurons, which caused and maintained NP pathological process [43]. Therefore, intrathecal injection of TRESK overexpression adenovirus in the early phase of NP and continuous injection were administrated in our study. The results showed inhibition of TRESK downregulation induced by SNI could obviously reduce gliocytes activation and gap junctions upregulation in spinal cord of rats, thereby achieving the effect for treatment of NP.

In summary, the present study unveiled the relationship of DRG and spinal cord with the distribution of TRESK, which was expressed in neurons rather than gliocytes. Intrathecal administration of TRESK-overexpressing adenovirus could alleviate the hyperalgesia induced by SNI via the inhibition of gliocyte activation and gap junctions upregulation. TRESK mediate gap junctions upregulation and gliocyte activation involves in the pathogenesis of NP, which might bring prospects in clinical therapeutics for NP and pain management.

Acknowledgements This project was supported by Grants from National Natural Science Foundation of China (81300974), the Natural Science Foundation of Guangdong Province (2015A030313899) and the Medical Scientific Research Foundation of Guangdong Province (A2015013).

Compliance with Ethical Standards

Conflict of interest The authors declare no conflicts of interest.

References

1. Gilron I, Baron R, Jensen T (2015) Neuropathic pain: principles of diagnosis and treatment. Mayo Clin Proc 90(4):532–545
2. Thibault K, Calvino B, Dubacq S, Roualle-de-Rouville M, Sordoillet V, Rivals I, Pezet S (2012) Cortical effect of oxaliplatin associated with sustained neuropathic pain: exacerbation of cortical activity and down-regulation of potassium channel expression in somatosensory cortex. Pain 153(8):1636–1647
3. Liu CY, Lu ZY, Li N, Yu LH, Zhao YF, Ma B (2015) The role of large-conductance, calcium-activated potassium channels in a rat model of trigeminal neuropathic pain. Cephalalgia 35(1):16–35
4. Tulleuda A, Cokic B, Callejo G, Saiani B, Serra J, Gasull X.TRESK channel contribution to nociceptive sensory neurons excitability: modulation by nerve injury (2011) Mol Pain 7:30

5. Enyedi P, Czirják G (2010) Molecular background of leak K + currents: two-pore domain potassium channels. Physiol Rev 90(2):559–605
6. Liu C, Au JD, Zou HL, Cotten JF, Yost CS (2004) Potent activation of the human tandem pore domain K channel TRESK with clinical concentrations of volatile anesthetics. Anesth Analg 99(6):1715–1722
7. Pollema-Mays SL, Centeno MV, Ashford CJ, Apkarian AV, Martina M (2013) Expression of background potassium channels in rat DRG is cell-specific and down-regulated in a neuropathic pain model. Mol Cell Neurosci 57:1–9
8. Clark AK, Yip PK, Malcangio M (2009) The liberation of fractalkine in the dorsal horn requires microglial cathepsin S. J Neurosci 29(21):6945–6954
9. Zhuang ZY, Gerner P, Woolf CJ, Ji RR (2005) ERK is sequentially activated in neurons, microglia, and astrocytes by spinal nerve ligation and contributes to mechanical allodynia in this neuropathic pain model. Pain 114(1–2):149–159
10. Zhuang ZY, Wen YR, Zhang DR et al (2006) A peptide c-Jun N-terminal kinase (JNK) inhibitor blocks mechanical allodynia after spinal nerve ligation: respective roles of JNK activation in primary sensory neurons and spinal astrocytes for neuropathic pain development and maintenance. J Neurosci 26(13):3551–3560
11. Tsuda M, Kohro Y, Yano T et al (2011) JAK-STAT3 pathway regulates spinal astrocyte proliferation and neuropathic pain maintenance in rats. Brain 134(Pt4):1127–1139
12. Jeon YH, Youn DH (2015) Spinal gap junction channels in neuropathic pain. Korean. J Pain 28(4):231–235
13. Hwang HY, Zhang E, Park S, Chung W, Lee S, Kim DW, Ko Y, Lee W (2015) TWIK-related spinal cord K+ channel expression is increased in the spinal dorsal horn after spinal nerve ligation. Yonsei Med J 56(5):1307–1315
14. Söhl G, Maxeiner S, Willecke K (2005) Expression and functions of neuronal gap junctions. Nat Rev Neurosci 6(3):191–200
15. Chapman RJ, Lall VK, Maxeiner S, Willecke K, Deuchars J, King AE (2013) Localization of neurones expressing the gap junction protein Connexin45 within the adult spinal dorsal horn: a study using Cx45-eGFP reporter mice. Brain Struct Funct 218(3):751–765
16. Lee IH, Lindqvist E, Kiehn O, Widenfalk J, Olson L (2005) Glial and neuronal connexin expression patterns in the rat spinal cord during development and following injury. J Comp Neurol 489(1):1–10
17. Zhou J, Yao SL, Yang CX, Zhong JY, Wang HB, Zhang Y (2012) TRESK gene recombinant adenovirus vector inhibits capsaicin-mediated substance P release from cultured rat dorsal root ganglion neurons. Mol Med Rep 5(4):1049–1052
18. Zhou J, Yang CX, Zhong JY, Wang HB (2013) Intrathecal TRESK gene recombinant adenovirus attenuates spared nerve injury-induced neuropathic pain in rats. Neuroreport 24(3):131–136
19. Yaksh TL, Rudy TA (1976) Chronic catheterization of the spinal subarachnoid space. Physiol Behav 17(6):1031–1036
20. Decosterd I, Woolf CJ (2000) Spared nerve injury: an animal model of persistent peripheral neuropathic pain. Pain 87(2):149–158
21. Bourquin AF, Süveges M, Pertin M, Gilliard N, Sardy S, Davison AC, Spahn DR, Decosterd I (2006) Assessment and analysis of mechanical allodynia-like behavior induced by spared nerve injury (SNI) in the mouse. Pain 122(1–2):14.e1-14
22. Chaplan SR, Bach FW, Pogrel JW, Chung JM, Yaksh TL (1994) Quantitative assessment of tactile allodynia in the rat paw. J Neurosci Methods 53(1):55–63
23. Hargreaves K, Dubner R, Brown F, Flores C, Joris J (1988) A new and sensitive method for measuring thermal nociception in cutaneous hyperalgesia. Pain 32(1):77–88
24. Jiao XC, Zhang HR, Zhang X, et al (2014) Research progress in interactions between neuron and satellite glial cell. Chin Pharmacol Bull 30(5):612–614
25. Warwick RA, Hanani M (2013) The contribution of satellite glial cells to chemotheraphy-induced neuropathic pain. Eur J Pain 17(4):571–580
26. Guo Z, Cao YQ (2014) Over-expression of TRESK K(+) channels reduces the excitability of trigeminal ganglion nociceptors. PLoS ONE 9(1):e87029
27. Marsh B, Acosta C, Djouhri L, Lawson SN (2012) Leak K + channel mRNAs in dorsal root ganglia: relation to inflammation and spontaneous pain behaviour. Mol Cell Neurosci 49(3):375–386
28. Kollert S, Dombert B, Döring F, Wischmeyer E (2015) Activation of TRESK channels by the inflammatory mediator lysophosphatidic acid balances nociceptive signalling. Sci Rep 5:12548
29. Watkins LR, Milligan ED, Maier SF (2001) Glial activation: a driving force for pathological pain. Trends Neurosci 24(8):450–455
30. Loggia ML, Chonde DB, Akeju O et al (2015) Evidence for brain glial activation in chronic pain patients. Brain 138(Pt3):604–615
31. Del Valle L, Schwartzman RJ, Alexander G (2009) Spinal cord histopathological alterations in a patient with longstanding complex regional pain syndrome. Brain Behav Immun 23(1):85–91
32. Sonekatsu M, Taniguchi W, Yamanaka M, Nishio N, Tsutsui S, Yamada H, Yoshida M, Nakatsuka T (2016) Interferon-gamma potentiates NMDA receptor signaling in spinal dorsal horn neurons via microglia-neuron interaction. Mol Pain 12
33. Chen MJ, Kress B, Han X, Moll K, Peng W, Ji RR, Nedergaard M (2012) Astrocytic CX43 hemichannels and gap junctions play a crucial role in development of chronic neuropathic pain following spinal cord injury. Glia 60(11):1660–1670
34. Wu A, Green CR, Rupenthal ID, Moalem-Taylor G (2012) Role of gap junctions in chronic pain. J Neurosci Res 90(2):337–345
35. Takeuchi H, Suzumura A (2014) Gap junctions and hemichannels composed of connexins: potential therapeutic targets for neurodegenerative diseases. Front Cell Neurosci 8:189
36. Retamal MA, Froger N, Palacios-Prado N, Ezan P, Sáez PJ, Sáez JC, Giaume C (2007) Cx43 hemichannels and gap junction channels in astrocytes are regulated oppositely by proinflammatory cytokines released from activated microglia. J Neurosci 27(50):13781–13792
37. Jin SX, Zhuang ZY, Woolf CJ, Ji RR (2003) p38 mitogen-activated protein kinase is activated after a spinal nerve ligation in spinal cord microglia and dorsal root ganglion neurons and contributes to the generation of neuropathic pain. J Neurosci 23(10):4017–4022
38. Nakamura Y, Morioka N, Zhang FF, Hisaoka-Nakashima K, Nakata Y (2015) Downregulation of connexin36 in mouse spinal dorsal horn neurons leads to mechanical allodynia. J Neurosci Res 93(4):584–591
39. Kay CW, Ursu D, Sher E, King AE (2016) The role of Cx36 and Cx43 in 4-aminopyridine-induced rhythmic activity in the spinal nociceptive dorsal horn: an electrophysiological study in vitro. Physiol Rep 4(14):e12852
40. Nakamura Y, Morioka N, Zhang FF, Hisaoka-Nakashima K, Nakata Y (2015) Downregulation of connexin36 in mouse spinal dorsal horn neurons leads to mechanical allodynia. J Neurosci Res 93:584–591
41. Xu Q, Cheong YK, He SQ, Tiwari V, Liu J, Wang Y et al (2014) Suppression of spinal connexin 43 expression attenuates mechanical hypersensitivity in rats after an L5 spinal nerve injury. Neurosci Lett 566:194–199

42. Yoon SY, Robinson CR, Zhang H et al (2013) Spinal astrocyte gap junctions contribute to oxaliplatin-induced mechanical hypersensitivity. J Pain 14(2):205–214
43. Roh DH, Yoon SY, Seo HS et al (2010) Intrathecal injection of carbenoxolone, a gap junction decoupler, attenuates the induction of below-level neuropathic pain after spinal cord injury in rats. Exp Neurol 224(1):123–132